Nuclear Instruments and Methods in Physics Research A 791 (2015) 65–68

Contents lists available at ScienceDirect

Nuclear Instruments and Methods in Physics Research A

journal homepage: www.elsevier.com/locate/nima

Comparison of light transport-incorporated MCNPX and FLUKA codes in generating organic scintillators responses to neutrons and gamma rays

M. Tajik, N. Ghal-Eh *

School of Physics, Damghan University, P.O. Box 36716-41167 Damghan, Iran

ARTICLE INFO

Article history:
Received 11 March 2015
Received in revised form
13 April 2015
Accepted 16 April 2015
Available online 25 April 2015

Keywords:
MCNPX
FLUKA
PHOTRACK
Scintillator
Response
Efficiency

ABSTRACT

The NE102 plastic scintillator response to ^{137}Cs gamma rays and NE213 liquid scintillator response to both mono-energetic and ^{241}Am–Be neutrons have been modeled using FLUKA's EVENTBIN and MCNPX's PTRAC cards. The comparison made in different energy regions confirms that the overall difference is less than 6%.

1. Introduction

The responses of organic scintillators are basically achievable either with stand-alone codes (e.g., SCINFUL [1], O5S [2], etc.) or with general-purpose codes (e.g., MCNPX [3], FLUKA [4], GEANT4 [5]). Although the first group is more user-friendly, their use is limited to a specific geometry, material and conditions. The second group codes can be utilized in variety of simulation problems but they normally require a good knowledge of the general-purpose code as well as an efficient post-processing program. The results of the second group are highly dependent on the cross-section libraries of the general-purpose code, hence, some differences may be seen between their results and both simulations and experimental studies.

The main purpose of the present study is to simulate the response of the scintillation detectors to neutrons and gamma-rays, however, since the MCNPX code does not model the optical photon transport and it has been decided not to use the light transport capabilities of FLUKA code, both the MCNPX and FLUKA codes have been chosen to transport the incident neutrons, gamma-rays, neutron-induced charged particles and fast electrons, whilst the light transport code PHOTRACK [6] has been incorporated through a post-processing FORTRAN program to produce the scintillator response.

2. Simulation studies

2.1. Deposition energy calculations with FLUKA and MCNPX

The organic scintillators and the radiation sources used in this study have been listed in Table 1. The FLUKA cards BEAM and BEAMPOS and the FORTRAN file SOURCE are responsible for introducing the energy type, position/direction and the energy spectrum of source particles, respectively. The FLUKA card EVENTBIN is used for partitioning the scintillator cell into a number of small voxels whose sizes must be comparable to the average mean free paths of the particles of interest in order to have an appropriate deposition energy estimate. Following the calculations of electron and proton ranges in scintillators, it has been decided to use 1000 and 512,000 voxels in NE102 and NE213 scintillators, respectively, which are corresponding to the ranges of highest-energy Compton electrons and recoiled protons as a result of ^{137}Cs gamma rays and Am–Be neutrons. The EVENTBIN output provides the user with the coordinates and deposition energies of every single source particle. Since the scintillation light produced as a result of neutron interaction with carbon nuclei is negligible when the neutron energy does not exceed 11 MeV [7], only the deposition energies of

* Corresponding author. Tel./fax: +98 23 35220090.
E-mail address: ghal-eh@du.ac.ir (N. Ghal-Eh).

http://dx.doi.org/10.1016/j.nima.2015.04.043
0168-9002/

Table 1
Scintillator sizes/types and radiation sources of the present study.

Scintillator type	Scintillator size	Radiation
NE102 (plastic)	5.08 cm diameter by 5.08 cm high cylinder	^{137}Cs gamma rays
NE213 (liquid)	4.65 cm diameter by 4.60 cm high cylinder	Mono-energetic neutrons
	5.08 cm diameter by 5.08 cm high cylinder	^{241}Am–Be neutrons

recoiled protons are taken. The scintillation light for the EVENTBIN data can be calculated using TCQUENCH card, which uses well-known Birks formula [8] for its calculations.

In the MCNPX code, the PTRAC card is capable of recording the coordinates and deposition energies of secondary charged particles. However, one has to extract the deposition energy data from the PTRAC card (normally by a post-processing program) as well as using energy-to-light conversion formulas (e.g., [9] and [10]) in order to calculate the scintillation light.

A comparison between the deposition energies calculated with MCNPX PTRAC and FLUKA EVENTBIN cards and also the subtraction plot for an NE102 scintillator exposed to ^{137}Cs gamma rays have been illustrated in Fig. 1. The plot shows the maximum agreement at the Compton edge. Fig. 2 also shows the comparison of the two codes in generating the energy distributions for NE213 scintillator exposed to mono-energetic (1, 3, 5, 7, 9 and 10 MeV) neutrons. The overall agreement between simulated NE213 scintillator responses with FLUKA and MCNPX codes is excellent however some discrepancies exist at lower light outputs (i.e., the region normally dominated by the scintillation lights of heavy charged particles such as carbon nuclei).

The total light outputs (area under the scintillator response shown in Fig. 2) calculated with FLUKA EVENTBIN and MCNPX PTRAC card have been compared in Table 2. From the good overall agreement one may conclude that the neutron interaction cross-sections are almost the same for these two codes in the neutron energy region shown in Fig. 2.

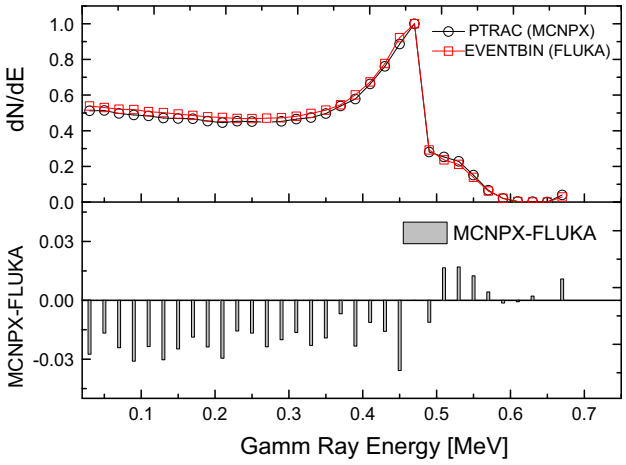

Fig. 1. The energy distribution of deposition energies calculated with MCNPX PTRAC and FLUKA EVENTBIN cards and the subtraction plot for an NE102 scintillator exposed to ^{137}Cs gamma rays.

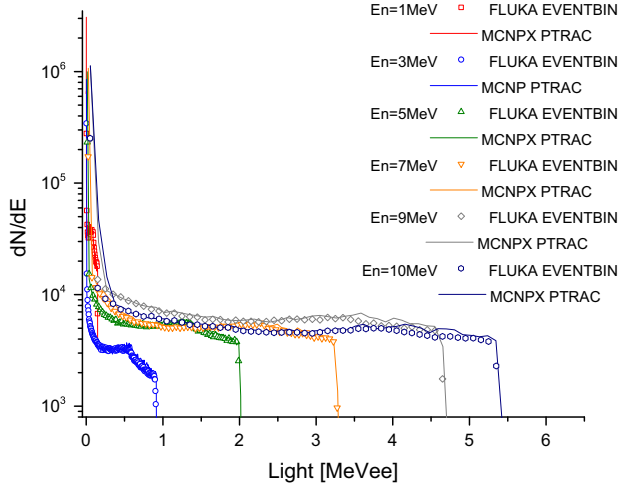

Fig. 2. Response of an NE213 scintillator when exposed to mono-energetic neutrons generated with FLUKA EVENTBIN and MCNPX PTRAC. The energy–to–light conversion factors are taken from the work of Verbinski et al. [9].

3. Light transport simulation with PHOTRACK

Having calculated the deposition energies and scintillation light, the full simulation of scintillator response requires a light transport modeling. The light transport simulation is extremely important when using large-sized scintillators, different shapes/sizes of lightguides and different painting configurations. Here, the Monte Carlo code, PHOTRACK [11], has been used for the light transport simulation part in the framework of a post-processing program [12]. PHOTRACK considers the wavelength dependencies, lightguide geometries, spatial variation of photocathode quantum efficiency, etc. The electronic noise and dynode chain contributions in the scintillator response which result in an extra broadening can be also included by convolving a random Gaussian broadening function [13].

4. Experimental studies

In order to verify the simulation studies of Section 2, an NE102 plastic scintillator of 5.08 cm diameter by 5.08 cm high cylinder attached to an XP202 PHOTONIS photomultiplier tube is exposed to a 12 μCi ^{137}Cs gamma ray source. Also, an NE213 scintillator of the same size and photomultiplier tube but with and without a 5 cm long plexiglass lightguide is exposed to 100 mCi Am–Be

Table 2
The comparison between the NE213 scintillator total light outputs calculated with FLUKA EVENTBIN and MCNPX PTRAC cards for different neutron energies.

Neutron energy (MeV)	Total light output difference (%)
1	5.18
3	1.52
5	1.01
7	4.32
9	6.89
10	10.65

source. The neutron source is far enough from the surrounding wall such that the backscattering effects are negligible.

Since almost all isotopic neutron sources emit gamma rays as well, one has to perform appropriate neutron-gamma discrimination (here, by using a zero-crossing method) in order to obtain pure neutron response. In this study, the neutron-gamma discrimination is undertaken by anode pulse, which simultaneously enters PSD and CFD modules. In PSD modules [14], the anode pulse becomes multipolar resulting in several zero-crossings. Every zero-crossing event generates a fast signal that is eventually fed into a TAC (time-to-amplitude convertor) module. The dynode output is amplified through the pre-amplifier and spectroscopy amplifier modules for required amplifications and shapings and then it is, simultaneously with the TAC output, fed into a similar ADC. The spectrum given by a multiparameter analyzer can now demonstrate both the pulse-height (i.e., energy) and the timing characteristics (i.e., particle type; neutrons or gamma-rays). The energy calibration is made by 1274 keV ^{22}Na gamma-rays to determine the variation of bias against the energy. The Compton edge of these gamma-rays is around 1061 keV, which is corresponding to 89% of the maximum count at the descending slope of the continuum.

The pure neutron response of an NE213 scintillator when exposed to Am–Be source and corresponding light-transport incorporated FLUKA and MCNPX simulations (using ISO 8529-1 Am–Be neutron spectrum (ISO, 2001 [15])) have been illustrated in Fig. 3. A small extra broadening has been added through a FORTRAN post–processing program using subroutine gasdev (introduced in [16]) to the simulation spectra for better matching with measured one. The broadening function used in this study has been previously measured by Green et al. [17], where for light values $L < 0.3$ MeVee and $L > 0.3$ MeVee, the broadening function varies as $16.22/L^{0.21}$ and $12.98/L^{0.44}$, respectively.

5. Results and discussion

The measured response function of a 5.08 cm by 5.08 cm cylindrical scintillator attached to 5.08 cm long polished lightguide when exposed to Am–Be neutron source has been compared with the corresponding simulation data generated with MCNPX-PHOTRACK and FLUKA-PHOTRACK hybrid codes in Fig. 3. Fig. 4 also illustrates a comparison between experimental data [9], SCINFUL results (as discussed in [12]) and two different hybrid

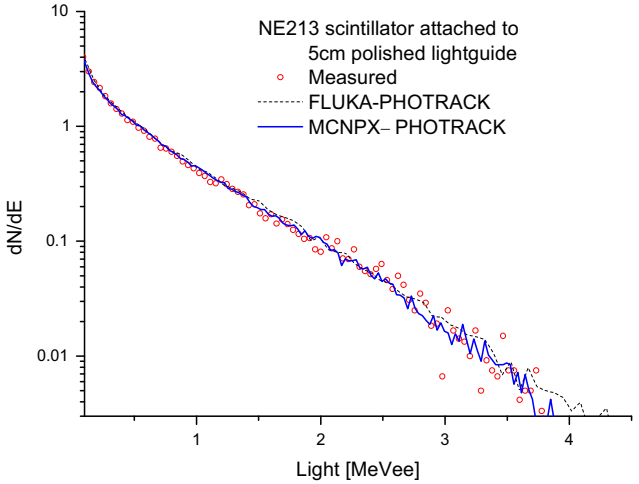

Fig. 3. The measured response of NE213 scintillator attached to 5 cm polished lightguide exposed to Am–Be source and corresponding light-transport incorporated FLUKA and MCNPX simulations.

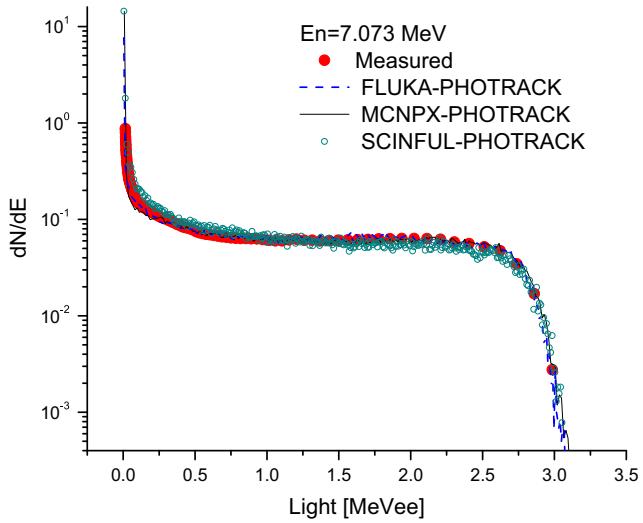

Fig. 4. NE213 responses to 7.073 MeV neutrons generated with light-transport incorporated codes (FLUKA, MCNPX and SCINFUL) and measurement data.

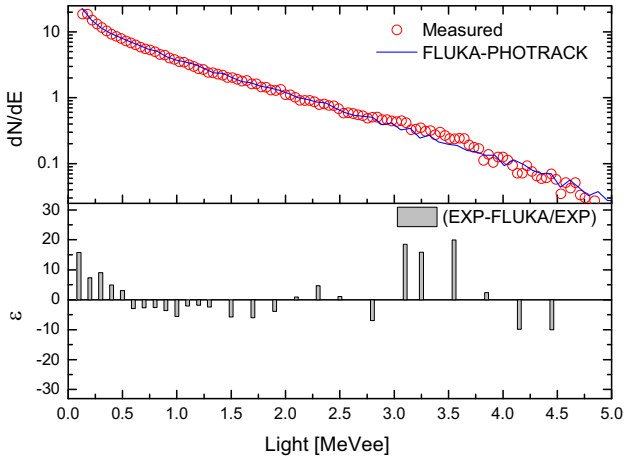

Fig. 5. The relative difference between experimental and FLUKA-PHOTRACK simulation data for a 2 inch by 2 inch right cylindrical NE213 scintillator exposed to an Am–Be source.

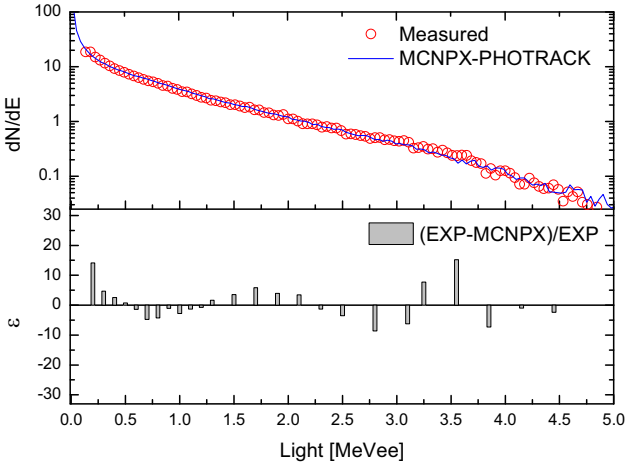

Fig. 6. The relative difference between experimental and MCNPX-PHOTRACK simulation data for a 2 inch by 2 inch right cylindrical NE213 scintillator exposed to an Am–Be source.

Table 3
The comparison between the areas under the Monte Carlo-generated and experimental responses of an NE213 scintillator when exposed to mono-energetic and Am–Be neutrons.

Neutron Source	Detector	Deviation from experimental data (%)		
		FLUKA-PHOTRACK	MCNPX-PHOTRACK	SCINFUL
Mono-energetic (7.073 MeV)	NE213 Scintillator 5.08 cm by 5.08 cm w/o lightguide	5.85	1.78	3.46
Am–Be	NE213 Scintillator 5.08 cm by 5.08 cm w/o lightguide	5.78	3.2	–
	NE213 Scintillator 5.08 cm by 5.08 cm w/ 5 cm lightguide	5.94	2.31	–

codes (FLUKA-PHOTRACK and MCNPX-PHOTRACK codes) responses for an NE213 scintillator when exposed to mono-energetic 7.073 MeV neutrons. The results confirm that all three codes are in a relatively good agreement except in low-pulse-height region. It is well-understood that higher pulse-height region corresponds to recoiled protons whilst the lower region may correspond to $^{12}C(n,\alpha)$, $^{12}C(n,3\alpha)$ and recoiled carbon nuclei [7]. Therefore, any difference in low amplitude region may be connected either to different cross-section libraries of neutron interactions for this energy region or the algorithms used for neutron interactions modeling.

In Figs. 5 and 6, the relative differences for the results of two hybrid codes, MCNPX-PHOTRACK and FLUKA-PHOTRACK, together with the measured response for a two-inch right cylinder NE213 scintillator when exposed to Am–Be neutrons have been shown for different energy regions. The ratio ε is defined as $(N_{exp}-N_{simul})/N_{exp}$, where N_{exp} and N_{simul} are the experimental and simulation counts for an energy interval, respectively.

The areas under the responses generated with light transport incorporated MCNPX and FLUKA codes compared with the corresponding measured data have been listed in Table 3. The maximum relative difference is less that 6%. As discussed earlier in this section, this difference may be corresponded to different cross-section libraries.

6. Concluding remarks

The event-by-event tracking feature of both MCNPX PTRAC and FLUKA EVENTBIN can be used to generate the responses of scintillation detectors to neutrons and gamma-rays. The scintillator response is obtained through the calculations of deposition energies left by neutron- and gamma-induced charged particles and the scintillation lights given by light curves (i.e., deposition energy-to-light conversion formulas). The scintillator responses generated with both MCNPX and FLUKA codes represents promising agreements with experimental data, except small discrepancies at low amplitudes.

References

[1] J.K. Dickens, SCINFUL: A Monte Carlo Based Computer Program to Determine a Scintillator Full Energy Response to Neutron Report ORNL-6463, Oak Ridge, United States, 1988.
[2] R.E. Textor, V.V. Verbinski, O5S: A Monte Carlo Code for Calculating the Pulse-Height Distributions Due to Mono-Energetic Neutrons on Organic Scintillators ORNL-4160, Oak Ridge National Laboratory, United States (1968) .
[3] J.S. Hendricks, et al., MCNPX 2.6.0 Extensions Report LA-UR-08-2216, Los Alamos National Laboratory, New Mexico, United States, 2008.
[4] T.T. Böhlen, F. Cerutti, M.P.W. Chin, A. Fassò, A. Ferrari, P.G. Ortega, A. Mairani, P.R. Sala, G. Smirnov, V. Vlachoudis, Nuclear Data Sheets 120 (2014) 211.
[5] S. Agostinelli, et al., Nuclear Instruments and Methods in Physics Research A A506 (2003) 250.
[6] N. Ghal-Eh, Radiation Physics and Chemistry 80 (2011) 365.
[7] M. Gohil, et al., Nuclear Instruments and Methods in Physics Research A A664 (2012) 304.
[8] J.B. Birks, The Theory and Practice of Scintillation Counting, Pergamon Press, Oxford, London, United Kingdom, 1964.
[9] V.V. Verbinski, et al., Nuclear Instruments and Methods in Physics Research A 65 (1968) 8.
[10] R.A. Cecil, B.D. Anderson, R. Madey, Nuclear Instruments and Methods in Physics Research A 161 (1979) 439.
[11] N. Ghal-Eh, M.C. Scott, R. Koohi-Fayegh, M.F. Rahimi, Nuclear Instruments and Methods in Physics Research A 516 (2004) 116.
[12] M. Tajik, N. Ghal–Eh, G.R. Etaati, H. Afarideh, Nuclear Instruments and Methods in Physics Research A 704 (2013) 104.
[13] M. Ranjbar Kohan, G.R. Etaati, N. Ghal-Eh, M.J. Safari, H. Afarideh, E. Asadi, Applied Radiation and Isotopes 70 (2012) 864.
[14] E. Bayat, N. Divani-Vais, M.M. Firoozabadi, N. Ghal-Eh, Radiation Physics and Chemistry 81 (2012) 217.
[15] International Standards Organization, Reference Neutron Radiations-Part 1: Characteristics and Methods of Production ISO-8529-1, International Organization for Standardization, Geneva, Switzerland, 2001.
[16] W.H. Press, S.A. Teukolsky, W.T. Vetterling, B.P. Flannery, 2nd ed.,Numerical Recipes in Fortran, 77, Cambridge University Press, Cambridge, England, 1992.
[17] S. Green, M.C. Scott, R. Koohi-Fayegh, A User Guide for the NPL NE213 Neutron Spectroscopy System, School of Physics and Astronomy, The University of Birmingham, UK, 1991.